Article

AQP2-induced acceleration of renal cell proliferation involves the activation of a regulatory volume increase mechanism dependent on NHE2†

Running head: NHE2-dependent RVI and AQP2-rised cell growth

Valeria Rivarola[1]*, Gisela Di Giusto[1], María José Christensen[1], Paula Ford[1] and Claudia Capurro[1]

[1]*Laboratorio de Biomembranas, IFIBIO Houssay, CONICET-UBA, Departamento de Ciencia Fisiológicas, Facultad de Medicina, Universidad de Buenos Aires, Argentina.*

Correspondence to: Dr. Valeria Rivarola, Ph.D. Laboratorio de Biomembranas, *IFIBIO Houssay, CONICET-UBA*, Departamento de Ciencias Fisiológicas. Facultad de Medicina, Universidad de Buenos Aires. Paraguay 2155 piso 7 (C1121ABG) Buenos Aires, ARGENTINA. TEL: 54-11-59509500 (Phone ext. 2145). e-mail: *vrivarola@yahoo.com*

Keywords: A quaporin 2; Na/H e xchanger; R egulatory volume increas e; Cell proliferation

Grant info rmation: This work was supported by grants from Fondo Nacional para la Ciencia y la Tecnología, Argentina; Grant Number: PICT 12-0750. Universidad de Buenos Aires, Argentina; Grant Number: UBACYT 20020100100648 and UBACYT 20020130100697. Consejo Nacional de Ciencia y Tecnología, Argentina; Grant Number: PIP 0088 and PIP 0296.

Received 20 October 2015; Revised 6 May 2016; Accepted 17 May 2016
Journal of Cellular Biochemistry

DOI 10.1002/jcb.25602

Abstract

We have previously shown in renal cells that expression of the water channel Aquaporin 2 (AQP2) increases the rate of cell proliferation by shortening the transit time through the S and G_2/M phases of the cell cycle. This acceleration is due, at least in part, to a down-regulation of regulatory volume decrease (RVD) mechanisms when volume needs to be increased in order to proceed into the S phase. We hypothesize that in order to increase cell volume, RVD mechanisms may be overtaken by regulatory volume increase mechanisms (RVI). In this study, we investigated if the isoform 2 of the Na^+/H^+ exchanger (NHE2), the main ion transporter involved in RVI responses, contributed to the AQP2-increased renal cell proliferation. Three cortical collecting duct cell lines were used: WT-$RCCD_1$ (not expressing AQPs), AQP2-$RCCD_1$ (transfected with AQP2) and mpkCCD_{c14} (with inducible AQP2 expression). We here demonstrate, for the first time, that both NHE2 protein activity and expression was increased in AQP2-expressing cells. NHE2 inhibition decreased cell proliferation and delayed cell cycle progression by slowing S and G_2/M phases only if AQP2 is expressed. Finally, we observed that only in AQP2-expressing cells a NHE2-dependent RVI response was activated in the S phase. These observations suggest that the AQP2-increased proliferation involves the activation of a regulatory volume increase mechanism dependent on NHE2. Therefore, we propose that the accelerated proliferation of AQP2-expressing cells requires a coordinated modulation of the RVD/RVI activity that contributes to cell volume changes during cell cycle progression.

This article is protected by copyright. All rights reserved

The Na^+/H^+ exchanger (NHE) plays an important role in a remarkable assortment of physiological processes, ranging from intracellular pH (pH_i) homeostasis and epithelial salt transport, to cellular volume regulation and cell proliferation [Donowitz et al., 2013; Fuster and Alexander, 2014; Orlowski and Grinstein, 2011]. Some of these events, such as cell proliferation, are closely associated with changes in cell volume [Lang et al., 2005; Lang et al., 2000]. In fact, previous reports indicate that factors that affect cell volume also have an effect on mechanisms that control cellular proliferation [Kunzelmann, 2005; Rouzaire-Dubois and Dubois, 1998]. It is well accepted that during progression through the cell cycle, cellular volume increases as a result of the accumulation of diverse substrates, protein synthesis and DNA duplication [Kunzelmann, 2005]. This cell volume increase may be achieved by inhibition of regulatory volume decrease mechanisms (RVD) and/or by activation of regulatory volume increase (RVI) mechanisms. In line with this proposal, several reports demonstrate that, in many cell types, RVI mechanisms are up regulated during cell growth [Lang et al., 1991; Lang et al., 1998b; Ritter and Wöll, 1996] and that RVD capacity is actively modulated throughout the cell cycle [Chen et al., 2002; Di Giusto et al., 2012; Wang et al., 2002]. Other reports, in tumor ras-oncogene-expressing cells, suggest that both RVD and RVI mechanisms are necessary for cell cycle progression [Lang et al., 1998a; Ritter and Wöll, 1996]. Therefore, evidence indicates that cellular proliferation requires mechanisms for cell volume regulation, and thus the movement of ions and water. However, little is known regarding the sequence of events leading from cell volume changes to cell cycle progression.

The water channels Aquaporins (AQPs) have been proposed to play a key role not only in the control of cell volume but also in cell migration, proliferation and apoptosis [Flamenco et al., 2009; Ford et al., 2005; Galan-Cobo et al., 2015; Galan-Cobo et al., 2016; Jablonski et al., 2004; Rivarola et al., 2010; Shimizu et al., 2014; Verkman, 2008]. In renal cells, we have demonstrated that AQP2 enhances cell proliferation rate by a coordinate activation of specific RVD mechanisms in the G_1 phase and their subsequent inhibition in the S phase of the cell cycle [Di Giusto et al., 2012]. What still remains unclear is whether activation of RVI mechanisms is also required to increase cell volume.

RVI is mainly accomplished by cellular NaCl uptake (Na^+/H^+ and Cl^-/HCO_3^- exchangers acting in parallel) and the obligated water influx that leads to cell swelling [Lang et al., 2007]. Although to date four different NHEs isoforms have already been described in epithelia (NHE1-4), in renal cells NHE2 is the isoform proposed to be involved in cell volume increase. It has been demonstrated that hyperosmolality increases its mRNA expression [Soleimani et al., 1994]. Moreover, our group previously demonstrated that a hypertonic shock activates NHE2 function [Ford et al., 2002]. Bearing in mind these observations and those showing that NHE2 favors cell growth in CHO cells [Kapus et al., 1994], the aim of the present study was to investigate the putative link between AQP2 expression, NHE2 function and RVI response during cell cycle progression. For this purpose, we used three renal cortical collecting duct cell lines: WT-$RCCD_1$ that do not express renal aquaporins (AQPs), AQP2-$RCCD_1$ that constitutively expresses AQP2 in the apical plasma membrane [Capurro et al., 2001; Ford et al., 2005] and mpkCCD_{c14} cells that modulate

AQP2 expression upon exposure to AVP or its analogues [Hasler et al., 2002]. Our results showed that AQP2-expressing cells have a higher basal pH_i, together with an increased NHE2 expression and increased NHE2 activity. In addition, only in the presence of AQP2, the inhibition of NHE2 reduced cell proliferation by slowing the transit through S and G_2/M phases of the cell cycle. In S phase, an activation of a NHE2-mediated RVI response was observed only in AQP2-expressing cells. These results indicate that NHE2 and AQP2 would work in coordination as part of the cellular device that regulates collecting duct cell cycle progression.

Materials and Methods

Cell culture

$RCCD_1$ cells (established by Dr. Marcel Blot-Chabaud in 1996), an epithelial cell line derived from rat renal cortical collecting duct, which maintains very high transepithelial resistance similar to that observed in the native tissue [Blot-Chabaud et al., 1996]. Two types of $RCCD_1$ cells were used: WT-$RCCD_1$ cells, which do not express aquaporin water channels [Capurro et al., 2001] and AQP2-$RCCD_1$ cells, stably transfected with cDNA coding for rat AQP2 [Ford et al., 2005]. WT-$RCCD_1$ cells were grown in a modified-DMEM (DM) medium (Dulbecco´s modified Eagle´s medium/Ham´s F-12, 1:1 v/v; 14 mM $NaHCO_3$, 2 mM glutamine; 50 nM dexamethasone; 30 nM sodium selenite; 5 μg/mL insulin; 5 μg/mL transferrin; 10 ng/mL epidermal growth factor; 50 nM triiodothyronine; 100 U/mL penicillin-streptomycin; 20 mM Hepes; pH 7.4) and 2% fetal bovine serum (Invitrogen, San Diego, CA, USA) at 37°C in 5% CO_2/95% air atmosphere [Blot-Chabaud et al., 1996]. AQP2-$RCCD_1$ cells were maintained in DM medium containing Geneticin (200 μg/mL, Invitrogen) as previously

reported [Ford et al., 2005]. All experiments were performed on WT- and AQP2-$RCCD_1$ cells between the 20^{th} and 40^{th} passages.

The $mpkCCD_{c14}$ cells (provided by A. Vandewalle and M. Bens, Institut National de la Santé et de la Recherche Médicale, Paris, France) were grown in flasks (passage 20^{th} –30^{th}) in DM supplemented with 2% fetal calf serum (DM: DMEM-Ham's F12 at 1:1 vol/vol, 60 nM sodium selenate, 5 g/ml transferrin, 2 mM glutamine, 50 nM dexamethasone, 1 nM triiodothyronine,10 ng/ml epidermal growth factor, 5 g/ml insulin, 20 mM D-glucose, and 20 mM HEPES, pH 7.4) (4) at 37°C in 5% CO_2-95% air atmosphere.

Cell cycle synchronization

Cells were synchronized in the S phase of the cell cycle by the double-block technique, using thymidine as an inhibitor of DNA synthesis [Di Giusto et al., 2012; Harper, 2005]. WT-$RCCD_1$, AQP2-$RCCD_1$ cells or $mpkCCD_{c14}$ cells in exponential growth were first exposed for 12 h to 2 mM thymidine. Cells were then released in fresh media for another 12 h, later followed by a second thymidine block for another 12 h.

Cell growth measures

For cell number counting of WT- and AQP2-$RCCD_1$ cells were seeded on 24 polywell at 25 x 10^3 cells/ml densities, allowed to attach for 24 h and then were grown in the different experimental conditions.

For cell number counting of $mpkCCD_{c14}$ cells were seeded on 24 polywell at 2 x 10^3 cells/ml densities in the presence of vehicle (water) or 100 μM dibutyryl cyclic AMP (dbAMPc), allowed to attach for 24 h and then were grown in the different experimental conditions.

After incubation, cells were detached by trypsination, resuspended in PBS-trypan blue to exclude non-viable cells, and counted in a Neubauer hemocytometer.

Cell proliferation and cell cycle analysis by flow cytometry

For dual parameter flow cytometry cells were pulsed with 20 μM of the thymidine analog 5-Bromodeoxyuridine (BrdU, Sigma-Aldrich, St. Louis, USA) for 1 h. After removal of BrdU, cells were allowed to continue cycling in fresh media for a chase period of up to 6 h. Cells were then harvested and fixed in 70% ethanol. BrdU content was analyzed after DNA denaturation with 2N HCl plus 0.1% Triton X-100 at room temperature followed by neutralization with 0.1 M $Na_2B_4O_7$ buffer, pH 8.5. The cells were labeled using specific anti-BrdU monoclonal antibodies (BD Biosciences, California, USA) and Cy2-conjugated secondary antibodies (Jackson Immuno, Pennsylvania, USA) and suspended in the presence of propidium iodide (PI, 50 μg/ml) and RNase A (1 mg/ml) in PBS for up to 4 h at 4°C in the dark. Bivariate histograms of BrdU/DNA content were obtained collecting Cy2 green fluorescence as a measure of $BrdU^+$ cells (log scale) and red PI fluorescence as a measure of DNA content (linear scale) for 30000 events in each sample using a FACS Calibur flow cytometer (Becton-Dickinson, California, USA). Cell cycle compartments were calculated from bivariate histograms after doublets exclusion (Win MDI 2.8 Joseph Trotter, The Scripps Research Institute, California, USA). The transit times through the S phase (T_s) and the G_2/M phase ($T_{G2/M}$) were calculated as previously described [Baron and Penit, 1990; Begg et al., 1985].

Cell surface biotinylation

90-95% confluent WT-RCCD$_1$, AQP2-RCCD$_1$ cells or mpkCCD$_{c14}$ cells grown for 4 days in the presence of vehicle (-AQP2) or 100 μM dbAMPc (+AQP2) were washed three times in cold PBS and cell surface biotinylation was performed with a Cell Surface Protein Isolation kit (Pierce, Illinois, USA) following the manufacturer's instructions. Briefly, the cells were rinsed with PBS and then biotinylated using EZ-Link Sulfo-NHS-SS-Biotin in PBS for 30 min on ice. After quenching, the cells were harvested and solubilized in Lysis Buffer and incubated for 30 min on ice. After centrifugation at 10,000 x g for 2 min at 4°C, the supernatant was added to Immobilized NeutrAvidin™ gel and incubated for 60 min at room temperature. After being washed, the biotinylated proteins were eluted in SDS/PAGE sample buffer containing 50 mM dithiothreitol.

Western blot studies

Immunoblotting experiments were carried out as previously described [Rivarola et al., 2010]. Briefly, total cell lysates or cell surface biotinylated membranes were subjected to 7.5 % SDS-polyacriylamide minigels electrophoresis using the Tris-Tricine buffer system and then transferred to nitrocellulose membranes (Mini Protean II, Bio-Rad, Hercules, CA, USA). Blots were blocked with 1% BSA and then probed using either rabbit polyclonal anti-NHE2 (dilution 1:300, Alfa Diagnostics International, Texas, USA), rabbit polyclonal anti-AQP2 (dilution 1:1000) generated against a peptide corresponding to amino acids 250-271 of rat AQP2, conjugated with keyhole limpet hemocyanin [Shi et al., 2001] or streptavidin-HRP (dilution 1:6000 DakoCytomation, Denmark). After being rinsed with PBS-Tween, membranes

were incubated with the appropriate secondary antibody (anti rabbit or anti mouse IgG conjugated to horseradish peroxidase, dilution 1:25000, Sigma-Aldrich A0545) and visualized using the chemiluminescence method (SuperSignal Substrate, Pierce). For densitometric quantification of biotinylated membranes from WT- and AQP2-RCCD$_1$ cells or –AQP2 and +AQP2 mpkCCD$_{c14}$ cells, samples were run in the same gel. Images were captured on a G:BOX (Syngene, Maryland, USA) and the bands corresponding to AQP2 (29kDa), NHE2 (100 kDa) or streptavidin-HRP biotinylated protein (150 kDa band) were quantified by a densitometric analysis using Gel-Pro Analyzer software (Media Cybernetics, Maryland, USA) and expressed as the NHE2/streptavidin ratio.

Quantification of plasma membrane NHE2 by immunofluorescence studies

To quantify NHE2 proteins at the plasma membrane (PM) in RCCD$_1$ cells, immunofluorescence studies were performed. WT- or AQP2-RCCD$_1$ cells were seeded on coverslips and allowed to grow. Then monolayers were incubated with the specific plasma membrane marker Alexa 488-conjugated wheat germ agglutinin (WGA; Molecular Probes - Thermo Fisher Scientific, Massachusetts, USA) for 30 min at 4°C to label the surface glycoproteins. Cells were then fixed in 3% paraformaldehyde for 30 min and then permeabilized with 0.2% Triton X-100 at room temperature. Samples were sequentially incubated with polyclonal anti-rat NHE2 (dilution 1:50, Santa Cruz Biotechnology sc-30167) ON at 4ºC and secondary antibodies (rabbit anti-Cy3 conjugate, dilution 1:100, Jackson Immuno 111-165-003) for 2 h at room temperature. Then, nuclei were stained with Hoechst (5 µg/ml) for 1 min. Coverslips were mounted with

Vectashield mounting medium. Images were captured using epifluorescence on an Olympus FluoView FV1000 confocal microscope and digitalized.

For quantification of NHE2 at the plasma membrane we create a mask of the plasma membrane as previously described [Janecki et al., 2000]. Briefly, we used Image-J software as follows: WGA images were binarized so that the signal from WGA was ascribed the value of "1" and the remainder of the image was ascribed the value of "0". The Boolean logical operation "AND" was then performed on the corresponding images, representing signals from NHE2-Cy3 and from WGA (binary mask). This resulted in generation of a new image in which only the NHE2-Cy3 fluorescent signal corresponding to the PM was present. The intensity of NHE2-Cy3 fluorescence corresponding to the PM was quantified by densitometry using Image-J software and then analyzed using the formula:

$$\sum_{n} IF_{PM}(n)$$

In which n stands for the number of optical sections required to scan the entire cell, and IF_{PM} (n) stand for integrated fluorescence intensity of the plasma membrane within a given optical section. Plasma membrane NHE2 fluorescence was finally normalized to the number of cells per field.

Intracellular pH studies

$RCCD_1$ monolayers, grown on permeable filters, were inserted between two lucite frames, separating two fluid compartments when diagonally placed in a quartz cuvette with control solution (Table 1) as previously reported [Ford et al., 2002]. Free access both to the apical and basolateral baths was possible. Measurements were made with a computerized and thermoregulated (37°C) spectrofluorometer (Jasco 770, Maryland, USA). For measurements, the cell

monolayer was placed forming a 45° angle with the exploring beam. Fluorescence emission was monitored at 535 nm, with excitation wavelengths of 439 and 510 nm. For intracellular pH (pH_i) measurements cells were loaded with 8 μM of 2',7'bis(2-carboxyethyl)-5-(and–6) carboxyfluorescein acetoxymethyl ester (BCECF/AM, Molecular Probes) during 60 min at 37°C, both from the apical and basolateral baths. The ratio of the BCECF fluorescence emitted from dye-loaded cells was calibrated, in terms of pH, by incubating the cells in "high K^+ solution" (140 mM KCl, 4.6 mM NaCl, 1 mM $MgCl_2$, 2 mM $CaCl_2$, 10 mM Hepes, 5 mM glucose) and then by permeabilizing the cells with 5 μM nigericin to balance extracellular pH (pH_o) with pH_i. Then pH-bathing solution was stepped between 6.6 and 8.5. The 510 / 439 ratio was linear over this pH range (r = 0.99, n = 6).

In some experiments, NHE activity was monitored evaluating pH_i recovery after an acid load by the NH_4Cl pre-pulse technique as previously described [Ford et al., 2002]. The cells were exposed to control solution. Then to a 20 mM NH_4Cl pulse (NH_4Cl in Table 1), followed by Na^+ removal (0 Na^+ in Table 1). Then, Na^+ was restituted to the bath and Na^+-dependent pH_i recovery mechanisms were evaluated. Then acid fluxes were calculated as:

$$JH = \beta i \times \frac{dpH}{dt}$$

were J_{H^+} is the H^+ flux, dpH/dt is the rate of recovery from the acid load and β_i is the intracellular buffering power.

Intracellular H^+ buffering power (β_i) was estimated using application of external permeant weak bases as described by Roos and Boron [Roos and Boron, 1981]. In the present work we used application and removal of

NH_4Cl. This agent freely permeates the cell membrane in its uncharged form but exist mainly in ionized form once inside the cell. The ionization of a weak base absorbs H^+ ions. NH_4Cl can therefore be used to induce changes of pH_i which can then be used to estimate β_i following:

$$\beta i(mM) = \frac{[Hi]}{\Delta pHi}$$

were $[H^+]_i$ (mM) is the concentration of alkali (per litre of cytoplasm) introduced into the cell and ΔpH_i is the resulting change of pHi. $[H^+]_I$ is assumed to equal the intracellular concentration of NH_4^+ ions at the moment of their removal from the external solution. $[NH_4^+]_i$ at the moment of removal is given by:

$$[NH_4]_i(mM) = [NH_4]_o \cdot 10^{(pHo-pHi)}$$

Where $[NH_4^+]_0$ is calculated from the total concentration of external NH_4Cl ($[NH_4Cl]$) and its pK using a rearrangement of the Henderson-Hasselbalch equation:

$$[NH_4]_o(mM) = \frac{[NH_4Cl]}{10^{(pHo-pk)}+1}$$

Measurement of regulatory volume increase activity

To determine the regulatory volume increase (RVI) activity WT-$RCCD_1$, AQP2-$RCCD_1$ or $mpkCCD_{c14}$ cells (stimulated or not with 100 μM dbAMPc) were seeded on culture flasks, either allowed to grow freely or synchronized. Cells were harvested by trypsinization with Trypsin/EDTA, washed in an isosmotic solution and then incubated for up to 10 min in the desired solution. Cells were incubated either in an isosmotic solution (311 ± 5 mOsM) containing (in mM): 90 NaCl, 10 $NaHCO_3$, 5 KCl, 1 $CaCl_2$, 0.8 $MgSO_4$, 1 $MgCl_2$, 100 mannitol, 20 Hepes, 5 glucose or in a hypertonic solution (419 ± 5 mOsM)

prepared by mannitol addition to obtain the desired osmolality, while maintaining the ionic strength. Solutions osmolality were routinely measured in a pressure vapor osmometer (Vapro; Wescor, Logan, Utah, USA). All solutions were titrated to pH 7.40 using Tris (Sigma-Aldrich) and bubbled with atmospheric air.

Cell volume was estimated from suspended cells using a Scepter™ handheld automated cell counter (Millipore, Massachussets, USA) fitted with a 60 µm Scepter sensor and ScepterPro software. The Scepter uses a Coulter principle to generate a histogram of cell-volume distribution ranging from 0 to 24 pl [Winterberg et al., 2012; Xiao et al., 2012].

RVI at t = 10 to 20 min, associated with the volumetric response of cells exposed to hypertonic medium, was calculated using the following equation:

$$\%RVI = \left[\frac{\left(\frac{V}{V_0}\right)_{10} - \left(\frac{V}{V_0}\right)_{\min}}{1 - \left(\frac{V}{V_0}\right)_{\min}} \right] \times 100$$

where V_0 is the initial cell volume, V is the volume at time = 10 to 20 min. $(V/V_0)_{min}$ is the minimal value of V/V_0 attained during hypertonic shrinkage and $(V/V_0)_{10}$ represents the value of V/V_0 observed at time = 10-20 min. RVI thus denotes the magnitude of volume regulation at time = 10-20 min with 100% RVI indicating complete volume regulation and 0% indicating no volume regulation.

Statistics

Values were reported as mean ± SEM, and n is the number of experiments. Student's t Test for unpaired data was used. $p < 0.05$ was considered a significant difference.

Results

NHE2 activity and expression are increased in the presence of AQP2

The first set of experiments examined the consequences of AQP2 expression on NHE activity in $RCCD_1$ cells. Intracellular pH (pH_i) measurements were performed in monolayers grown on permeable filters using an HCO_3^--free medium (Control, Table 1) to minimize bicarbonate-transporting systems. Figure 1A shows that in AQP2-expressing cells basal pH_i was higher than in WT cells. We then investigated whether this alkalinization could be due to a higher NHE activity. Since we have previously reported that WT-$RCCD_1$ cells expresses two isoforms of the Na^+/H^+ exchanger (NHE1 and NHE2) [Ford et al., 2002] we used the highly specific inhibitor HOE-694 to identify the isoforms. The inhibitor HOE-694 at low doses (1 μM) inhibits NHE1, but not NHE2, while at higher doses (15 μM) block both isoforms [Counillon and Pouyssegur, 2000; Counillon et al., 1993]. Figure 1B shows that independently of AQP2 expression 1 μM HOE-694 did not affect basal pH_i, indicating that NHE1 does not contribute to basal pH_i. In contrast, 15 μM HOE-694 induced an acidification significantly higher in AQP2-expressing cells than in WT cells. These results suggest that the higher basal pH_i observed in AQP2-$RCCD_1$ cells could be explained by an increased NHE2 activity. We further evaluated this possibility analyzing the difference in the NHE1 and NHE2 activity between WT and AQP2-expressing cells by the NH_4Cl pre-pulse technique [Boron and De Weer, 1976]. Figures 1C and 1D show time-course experiments of pH_i evolution, using the NH_4Cl pre-pulse technique, in control conditions and in the presence of 1 μM or 15 μM HOE-694. It can be noted that both cell lines acidify to the same extent when NH_4Cl is washout (ΔpH_i WT: -0.33 ± 0.15 vs AQP2: -0.39 ± 0.08. ns, n=10). In

addition the intracellular Buffer power ($ß_i$), was not affected by the expression of AQP2 ($ß_i$, mM pH^{-1}, WT: 8.27 ± 2.29 vs AQP2: 7.61 ± 2. NS, n=10). NHE1 activity was estimated as the difference between the H^+-fluxes of experiments performed in the absence or presence of 1 μM HOE-694 and NHE2 activity as the difference between experiments performed in the presence of 1 μM and 15 μM HOE-694. It can be seen in Figure 1E that NHE1 activity was similar in both cell lines. However, in AQP2-expressing cells, NHE2 activity was significantly higher than in WT cells.

To investigate whether the increase in NHE2 activity of AQP2-expressing cells was parallel to a change in protein expression, immunoblots experiments were carried out on WT- and AQP2-$RCCD_1$ cell surface biotinylated membranes. Figure 2A illustrates that NHE2 was expressed in both cell lines; however, densitometric analysis showed that the ratio of NHE2/Streptavidin protein was higher in AQP2-expressing cells. We also performed immunoblots experiments using another cortical collecting duct cell model: $mpkCCD_{c14}$ cell line. In the absence of stimulation, $mpkCCD_{c14}$ cells do not express plasma membrane AQP2 but upon addition of vasopressin, or its analogues, cells translocate AQP2 to the apical membrane AQP2 [Hasler et al., 2002]. Figure 2B shows that +AQP2-$mpkCCD_{c14}$ cells not only express plasma membrane AQP2 but also increase NHE2 protein expression.

Cell membrane expression of NHE2 in $RCCD_1$ cells was confirmed by immunofluorescence experiments. Since we were interested in quantifying plasma membrane-associated NHE2, WGA, a plasma membrane marker, was added in the immunofluorescence experiments. We then created a mask to analyze NHE2 immunofluorescence associated with plasma membrane as

described in methods section [Janecki et al., 2000]. Figure 2C illustrates that in AQP2-expressing cells, the plasma membrane-associated NHE2 stain was more intense. Signal quantification confirmed higher levels of plasma membrane-associated NHE2 immunofluorescence in AQP2-expressing cells as compared to WT cells (Figure 2D).

Altogether, these results suggest that the basal alkalinization observed in AQP2-expressing cells is probably due to the higher membrane protein NHE2 expression that leads to the higher NHE2 activity of these cells.

NHE2 activity contributes to cell cycle progression in AQP2-expressing cells

We then investigated whether NHE2 increased activity in AQP2-expressing cells could be implicated in the enhanced cell proliferation observed in these cells. In order to study only NHE2 activity cells were grown under conditions where NHE1 is inhibited. For this, we used two experimental conditions, one, cells grown in the presence of 1 μM HOE-694, with NHE2 being the only active Na^+/H^+ isoform (+ NHE2) and the other, cells grown in the presence of 15 μM HOE-694, to also inhibit NHE2 (-NHE2). Our results showed that inhibition of NHE2 activity did not affect WT-$RCCD_1$ cell growth but did significantly reduce the number of AQP2-$RCCD_1$ cells to a level similar to that observed in WT cells (Figure 3A). Further studies assessed BrdU incorporation by flow cytometry analysis in order to evaluate the proliferation of growing cells (Figure 3B). Results showed that the percentage of BrdU positive cells ($BrdU^+$) was significantly reduced in the absence of NHE2 activity only in cells expressing AQP2.

We also evaluated the time course of growing cells using the mpkCCD$_{c14}$ cells. Our results showed that inhibition of NHE2 activity did not affect non stimulated mpkCCD$_{c14}$ cells (-AQP2) growth, but did significantly reduce the number of cell growth in mpkCCD$_{c14}$ expressing AQP2 (Figure 3C). These results confirm that independently of the cortical collecting duct cell model AQP2 expression *per se* plays a role in the increase of the rate of cell growth.

We then determined whether cell growth disparities could be due to differences in cell cycle progression. To evaluate the progression of RCCD$_1$ cell through the cell cycle we performed BrdU pulse-chase experiments. Figure 4A and C show that independently of NHE2 activity immediately after BrdU pulse most BrdU$^+$ cells are in the S phase in WT- and AQP2-RCCD$_1$ cells. Figure 4B and D shows that after 5 h chase in fresh medium the percentage of cells in S-phase decreased and cells reached the subsequent phases. However, WT cells have significantly fewer BrdU$^+$ cells in G1 phase and higher BrdU$^+$ cells in G2/M phase than AQP2-expressing cells. When NHE2 was inhibited (-NHE2) in WT cells the proportion of BrdU$^+$ cells in each phase of the cell cycle did not change. However, in AQP2-expressing cells, after NHE2 inhibition the proportion of BrdU$^+$ cells in G1 phase decreased.

We then used the BrdU pulse-chase results to calculate the duration of the S phase (T_s) and the duration of the G_2/M phase ($T_{G2/M}$) of the cell cycle. It can be observed in Figure 5A and B, that when NHE2 is active (+NHE2) T_s and $T_{G2/M}$ times were both shorter in AQP2-expressing cells, but they increased to levels similar to WT cells when NHE2 activity was blocked. Together these results demonstrate that NHE2 has an important role in AQP2-induced acceleration of cell proliferation.

NHE2-dependent RVI response is activated during the S phase of the cell cycle in AQP2-expressing cells

We then investigated whether the increased NHE2 activity and the higher cell proliferation rate observed in the presence of AQP2 were linked to changes in the capacity of cell volume regulation during cell cycle progression. RVI activity was measured as cell volume recovery in response to a hypertonic gradient (ΔOsM= +100 mOsM) in synchronized (most cells at S phase) and unsynchronized cells (most cells at G_1 phase). Figure 6 shows the time course of cell volume in WT- and AQP2-RCCD$_1$ cells during the hypertonic challenge. It can be noted that, independently of AQP2 expression, in G_1 phase cells shrank but failed to recover cell volume (Figure 6A). In contrast, at S phase only cells expressing AQP2 were able to recover cell volume (Figure 6B). Figure 6C illustrates the percentage of cell volume recovery 10-20 minutes after the hypertonic shock (%RVI). It can be observed that RVI machinery was inactive during G_1 phase in both cell lines, but only AQP2-expressing cells activated the RVI during S phase. We then performed experiments on mpkCCD$_{c14}$ cells expressing or not AQP2. Figure 6D shows that only in the S phase of AQP2-expressing mpkCCD$_{14}$, cells are able to activate the RVI machinery. Finally, we investigated whether this activation was dependent on NHE2 activity.

Our results in AQP2-expressing cells showed that the blockage of NHE2 activity with HOE-694 15 μM inhibited S phase-associated RVI (%RVI in S: +NHE2 = 34.08 ± 8.92 vs -NHE2 = 1.93 ± 1.40, $p< 0.01$ n=15). For mpkCCD$_{c14}$ cells grown expressing AQP2, the blockage of NHE2 activity with HOE-694 15 μM also inhibited S phase-associated RVI (%RVI in S: +NHE2 = 15.33 ± 2.90 vs -NHE2 = 0 ± 0.01, $p< 0.01$ n=6). Altogether, these results demonstrate that

the RVI machinery activated during S phase in AQP2 expressing cells involves NHE2 activity.

Discussion

Although the Na^+/H^+ exchanger has long been implicated in the control of cell proliferation, the specific mechanisms are not yet fully elucidated. To date most studies have focused in the participation of NHE1 isoform, having a permissive role rather than an obligatory signaling role *per se.* In fact, it appears that NHE1-induced changes in pH_i may contribute to modulation of cell proliferation [Fuster and Alexander, 2014; Putney et al., 2002]. However, some lines of evidence indicate that under certain conditions NHE2 is also able to support proliferation [Kapus et al., 1994]. Moreover, it has been described that growth factors modulate NHE2 expression and activity through specific domains [Levine et al., 1993; Nath et al., 1999; Xu et al., 2001]. Since cell cycle progression is dependent on an increase in cell volume, in part mediated via NHEs, and AQPs are involved in cell volume regulation [Ford et al., 2005; Galizia et al., 2008], in this study we analyzed if NHE2 could influence renal cell proliferation focusing on its relationship with AQP2 expression and cell volume regulation.

We here demonstrate, for the first time, that AQP2-expressing cells have both higher pH_i and higher protein levels of NHE2 than WT-$RCCD_1$ cells. As we have previously demonstrated that in these cells NHE2 is mainly involved in steady-state pH_i regulation [Ford et al., 2002], the increase in basal pH_i in AQP2 expressing cells could be explained by the increased NHE2 protein abundance that leads to a rise in NHE2 activity. We also show that the increased NHE2 expression in the presence of AQP2 seems to be characteristic of CCD cells

since stimulating AQP2 expression in another CCD cell line, the mpkCCD$_{c14}$ cells, NHE2 protein abundance also enhances. As it is well-known that in many systems increases in pH_i may accelerate cell proliferation by stimulating the synthesis of protein, RNA, and DNA [Schreiber, 2005], it is likely that a higher basal pH_i observed in AQP2 cells could act as a facilitator to initiate cell cycle. Our data support this hypothesis since AQP2-expressing cells presented a NHE2-sensitive increased proliferation and inhibition of NHE2 activity slowed down the progress through the S and G_2/M phase of the cell cycle.

However, an increase in pH_i is not the only factor that contributed to accelerate proliferation since we have previously shown that the accelerated proliferation rate seen in AQP2-expressing cells depends, at least in part, on an increase in cell volume and the capacity for RVD changes during the S phase [Di Giusto et al., 2012; Rivarola et al., 2010]. We here demonstrated that while there was no RVI activity in cells in G_1 phase, in S phase, AQP2-expressing cells had an NHE2-mediated RVI activity. The participation of NHE2 in RVI is in line with previous reports in the collecting duct showing that hyperosmolality increases NHE2 mRNA expression and that transcriptional regulation of the NHE2 gene is mediated by two osmotic response elements [Bai et al., 1999; Soleimani et al., 1994]. Moreover, our previous studies indicated that NHE2 was activated by tonicity [Ford et al., 2002].

What could be the interplay between AQP2 and NHE2 to contribute to cell proliferation? It has recently been described that AQP2 promotes cell migration and epithelial morphogenesis through interaction with β-integrins that are connected to the actin cytoskeleton [Chen et al., 2012; Tamma et al., 2011]. It has also been shown that both AQP2 and NHE2 proteins can interact with

cytoskeleton through binding to cytoskeletal protein α–spectrin [Chow et al., 1999; Noda et al., 2005]. So it is likely that the increased NHE2 activity and the NHE2 associated-RVI observed in the presence of the water channel AQP2 may be related to the fact that both proteins may form part of an interactome that process proliferative cues. In line with this it has recently been described that AQP1 and AQP3 overexpression accelerates the cell proliferation because affects the expression of key proteins for the cell cycle progression and contributes to cell volume changes needed for this process [Galan-Cobo et al., 2015; Galan-Cobo et al., 2016]. So it cannot be discarded that along with volume changes other proteins related to proliferation may also be modified in AQP2-expressing cells. Further experimental efforts are needed to address this complex interplay between AQP2 and RVI activity at each phase of the cell cycle.

In conclusion, our data show that, in collecting duct cells, the water channel AQP2 plays an important and novel role in regulating cell proliferation through modulating the activation of the RVI machinery during S phase, a mechanism that in turn depends on NHE2 activity. Clarification of the mechanisms governing cell volume control by AQP2 would be very important in learning about correct cellular function as well as about diseases associated with failure in AQP2 expression and alterations in cell proliferation as in the case of Insipidus Nephrogenic Diabetes induced by chronic lithium treatment.

Acknowledgments

The authors are grateful to Dr. Juerguen Puenter (Aventis Pharma Deutschland GmbH, Germany) who kindly provided us with the HOE-694 compound.

References

1. Bai L, Collins JF, Muller YL, Xu H, Kiela PR, Ghishan FK. 1999. Characterization of cis-elements required for osmotic response of rat Na(+)/H(+) exchanger-2 (NHE-2) gene. Am J Physiol 277:R1112-9.
2. Baron C, Penit C. 1990. Study of the thymocyte cell cycle by bivariate analysis of incorporated bromodeoxyuridine and DNA content. Eur J Immunol 20:1231-6.
3. Begg AC, McNally NJ, Shrieve DC, Karcher H. 1985. A method to measure the duration of DNA synthesis and the potential doubling time from a single sample. Cytometry 6:620-6.
4. Bens M, Vallet V, Cluzeaud F, Pascual-Letallec L, Kahn A, Rafestin-Oblin ME, Rossier BC, Vandewalle A. 1999. Corticosteroid-dependent sodium transport in a novel immortalized mouse collecting duct principal cell line. J Am Soc Nephrol 10:923-34.
5. Blot-Chabaud M, Laplace M, Cluzeaud F, Capurro C, Cassingena R, Vandewalle A, Farman N, Bonvalet JP. 1996. Characteristics of a rat cortical collecting duct cell line that maintains high transepithelial resistance. Kidney Int 50:367-76.
6. Boron WF, De Weer P. 1976. Intracellular pH transients in squid giant axons caused by CO2, NH3, and metabolic inhibitors. J Gen Physiol 67:91-112.
7. Capurro C, Rivarola V, Kierbel A, Escoubet B, Farman N, Blot-Chabaud M, Parisi M. 2001. Vasopressin regulates water flow in a rat cortical collecting duct cell line not containing known aquaporins. J Membr Biol 179:63-70.

8. Chen L, Wang L, Zhu L, Nie S, Zhang J, Zhong P, Cai B, Luo H, Jacob TJ. 2002. Cell cycle-dependent expression of volume-activated chloride currents in nasopharyngeal carcinoma cells. Am J Physiol Cell Physiol 283:C1313-23.
9. Chen Y, Rice W, Gu Z, Li J, Huang J, Brenner MB, Van Hoek A, Xiong J, Gundersen GG, Norman JC, Hsu VW, Fenton RA, Brown D, Lu HA. 2012. Aquaporin 2 promotes cell migration and epithelial morphogenesis. J Am Soc Nephrol 23:1506-17.
10. Chow CW, Woodside M, Demaurex N, Yu FH, Plant P, Rotin D, Grinstein S, Orlowski J. 1999. Proline-rich motifs of the Na+/H+ exchanger 2 isoform. Binding of Src homology domain 3 and role in apical targeting in epithelia. J Biol Chem 274:10481-8.
11. Counillon L, Pouyssegur J. 2000. The expanding family of eucaryotic Na(+)/H(+) exchangers. J Biol Chem 275:1-4.
12. Counillon L, Scholz W, Lang HJ, Pouyssegur J. 1993. Pharmacological characterization of stably transfected Na+/H+ antiporter isoforms using amiloride analogs and a new inhibitor exhibiting anti-ischemic properties. Mol Pharmacol 44:1041-5.
13. Di Giusto G, Flamenco P, Rivarola V, Fernandez J, Melamud L, Ford P, Capurro C. 2012. Aquaporin 2-increased renal cell proliferation is associated with cell volume regulation. J Cell Biochem 113:3721-9.
14. Donowitz M, Ming Tse C, Fuster D. 2013. SLC9/NHE gene family, a plasma membrane and organellar family of Na(+)/H(+) exchangers. Mol Aspects Med 34:236-51.

15. Flamenco P, Galizia L, Rivarola V, Fernandez J, Ford P, Capurro C. 2009. Role of AQP2 during apoptosis in cortical collecting duct cells. Biol Cell 101:237-50.
16. Ford P, Rivarola V, Chara O, Blot-Chabaud M, Cluzeaud F, Farman N, Parisi M, Capurro C. 2005. Volume regulation in cortical collecting duct cells: role of AQP2. Biol Cell 97:687-97.
17. Ford P, Rivarola V, Kierbel A, Chara O, Blot-Chabaud M, Farman N, Parisi M, Capurro C. 2002. Differential role of Na+/H+ exchange isoforms NHE-1 and NHE-2 in a rat cortical collecting duct cell line. J Membr Biol 190:117-25.
18. Fuster DG, Alexander RT. 2014. Traditional and emerging roles for the SLC9 Na(+)/H (+) exchangers. Pflugers Arch 466:61-76.
19. Galan-Cobo A, Ramirez-Lorca R, Serna A, Echevarria M. 2015. Overexpression of AQP3 Modifies the Cell Cycle and the Proliferation Rate of Mammalian Cells in Culture. PLoS One 10:e0137692.
20. Galan-Cobo A, Ramirez-Lorca R, Toledo-Aral JJ, Echevarria M. 2016. Aquaporin-1 plays important role in proliferation by affecting cell cycle progression. J Cell Physiol 231:243-56.
21. Galizia L, Flamenco MP, Rivarola V, Capurro C, Ford P. 2008. Role of AQP2 in activation of calcium entry by hypotonicity: implications in cell volume regulation. Am J Physiol Renal Physiol 294:F582-90.
22. Harper JV. 2005. Synchronization of cell populations in G1/S and G2/M phases of the cell cycle. Methods Mol Biol 296:157-66.
23. Hasler U, Mordasini D, Bens M, Bianchi M, Cluzeaud F, Rousselot M, Vandewalle A, Feraille E, Martin PY. 2002. Long term regulation of

aquaporin-2 expression in vasopressin-responsive renal collecting duct principal cells. J Biol Chem 277:10379-86.

24. Jablonski EM, Webb AN, McConnell NA, Riley MC, Hughes FM, Jr. 2004. Plasma membrane aquaporin activity can affect the rate of apoptosis but is inhibited after apoptotic volume decrease. Am J Physiol Cell Physiol 286:C975-85.
25. Janecki AJ, Janecki M, Akhter S, Donowitz M. 2000. Quantitation of plasma membrane expression of a fusion protein of Na/H exchanger NHE3 and green fluorescence protein (GFP) in living PS120 fibroblasts. J Histochem Cytochem 48:1479-92.
26. Kapus A, Grinstein S, Wasan S, Kandasamy R, Orlowski J. 1994. Functional characterization of three isoforms of the Na+/H+ exchanger stably expressed in Chinese hamster ovary cells. ATP dependence, osmotic sensitivity, and role in cell proliferation. J Biol Chem 269:23544-52.
27. Kunzelmann K. 2005. Ion channels and cancer. J Membr Biol 205:159-73.
28. Lang F, Busch GL, Ritter M, Volkl H, Waldegger S, Gulbins E, Haussinger D. 1998a. Functional significance of cell volume regulatory mechanisms. Physiol Rev 78:247-306.
29. Lang F, Foller M, Lang K, Lang P, Ritter M, Vereninov A, Szabo I, Huber SM, Gulbins E. 2007. Cell volume regulatory ion channels in cell proliferation and cell death. Methods Enzymol 428:209-25.

30. Lang F, Foller M, Lang KS, Lang PA, Ritter M, Gulbins E, Vereninov A, Huber SM. 2005. Ion channels in cell proliferation and apoptotic cell death. J Membr Biol 205:147-57.

31. Lang F, Friedrich F, Kahn E, Woll E, Hammerer M, Waldegger S, Maly K, Grunicke H. 1991. Bradykinin-induced oscillations of cell membrane potential in cells expressing the Ha-ras oncogene. J Biol Chem 266:4938-42.

32. Lang F, Lepple-Wienhues A, Paulmichl M, Szabó I, Siemen D, Gulbins E. 1998b. Ion channels, cell volume, and apoptotic cell death. Cell Physiol Biochem 8:285-292.

33. Lang F, Ritter M, Gamper N, Huber S, Fillon S, Tanneur V, Lepple-Wienhues A, Szabo I, Gulbins E. 2000. Cell volume in the regulation of cell proliferation and apoptotic cell death. Cell Physiol Biochem 10:417-28.

34. Levine SA, Montrose MH, Tse CM, Donowitz M. 1993. Kinetics and regulation of three cloned mammalian Na+/H+ exchangers stably expressed in a fibroblast cell line. J Biol Chem 268:25527-35.

35. Nath SK, Kambadur R, Yun CH, Donowitz M, Tse CM. 1999. NHE2 contains subdomains in the COOH terminus for growth factor and protein kinase regulation. Am J Physiol 276:C873-82.

36. Noda Y, Horikawa S, Katayama Y, Sasaki S. 2005. Identification of a multiprotein "motor" complex binding to water channel aquaporin-2. Biochem Biophys Res Commun 330:1041-7.

37. Orlowski J, Grinstein S. 2011. Na+/H+ exchangers. Compr Physiol 1:2083-100.

38. Putney LK, Denker SP, Barber DL. 2002. The changing face of the Na+/H+ exchanger, NHE1: structure, regulation, and cellular actions. Annu Rev Pharmacol Toxicol 42:527-52.

39. Ritter M, Wöll E. 1996. Modification of Cellular Ion Transport by the Ha-ras Oncogene: Steps towards Malignant Transformation. Cell Physiol Biochem 6:245-270.

40. Rivarola V, Flamenco P, Melamud L, Galizia L, Ford P, Capurro C. 2010. Adaptation to alkalosis induces cell cycle delay and apoptosis in cortical collecting duct cells: role of Aquaporin-2. J Cell Physiol 224:405-13.

41. Roos A, Boron WF. 1981. Intracellular pH. Physiol Rev 61:296-434.

42. Rouzaire-Dubois B, Dubois JM. 1998. K+ channel block-induced mammalian neuroblastoma cell swelling: a possible mechanism to influence proliferation. J Physiol 510 (Pt 1):93-102.

43. Schreiber R. 2005. Ca2+ signaling, intracellular pH and cell volume in cell proliferation. J Membr Biol 205:129-37.

44. Shi H, Levy-Holzman R, Cluzeaud F, Farman N, Garty H. 2001. Membrane topology and immunolocalization of CHIF in kidney and intestine. Am J Physiol Renal Physiol 280:F505-12.

45. Shimizu H, Shiozaki A, Ichikawa D, Fujiwara H, Konishi H, Ishii H, Komatsu S, Kubota T, Okamoto K, Kishimoto M, Otsuji E. 2014. The expression and role of Aquaporin 5 in esophageal squamous cell carcinoma. J Gastroenterol 49:655-66.

46. Soleimani M, Singh G, Bizal GL, Gullans SR, McAteer JA. 1994. Na+/H+ exchanger isoforms NHE-2 and NHE-1 in inner medullary collecting duct

cells. Expression, functional localization, and differential regulation. J Biol Chem 269:27973-8.

47. Tamma G, Lasorsa D, Ranieri M, Mastrofrancesco L, Valenti G, Svelto M. 2011. Integrin signaling modulates AQP2 trafficking via Arg-Gly-Asp (RGD) motif. Cell Physiol Biochem 27:739-48.
48. Verkman AS. 2008. Mammalian aquaporins: diverse physiological roles and potential clinical significance. Expert Rev Mol Med 10:e13.
49. Wang L, Chen L, Zhu L, Rawle M, Nie S, Zhang J, Ping Z, Kangrong C, Jacob TJ. 2002. Regulatory volume decrease is actively modulated during the cell cycle. J Cell Physiol 193:110-9.
50. Winterberg M, Rajendran E, Baumeister S, Bietz S, Kirk K, Lingelbach K. 2012. Chemical activation of a high-affinity glutamate transporter in human erythrocytes and its implications for malaria-parasite-induced glutamate uptake. Blood 119:3604-12.
51. Xiao F, Waldrop SL, Khimji AK, Kilic G. 2012. Pannexin1 contributes to pathophysiological ATP release in lipoapoptosis induced by saturated free fatty acids in liver cells. Am J Physiol Cell Physiol 303:C1034-44.
52. Xu H, Collins JF, Bai L, Kiela PR, Lynch RM, Ghishan FK. 2001. Epidermal growth factor regulation of rat NHE2 gene expression. Am J Physiol Cell Physiol 281:C504-13.

Table 1: Composition of solutions used for determination of pH_i recovery.

Solution	Control	NH_4Cl	0 Na^+
NaCl	147	127	----
Hepes	30	30	30
KCl	3	3	3
$CaCl_2$	1.8	1.8	1.8
$MgSO_4$	1	1	1
KH_2PO_4	1	1	1
K_2SO_4	1	1	1
NH_4Cl	----	20	----
TMA	----	----	147
glucose	5.6	5.6	5.6

All concentrations are given in mM; pH was adjusted to 7.4 at 37°C.

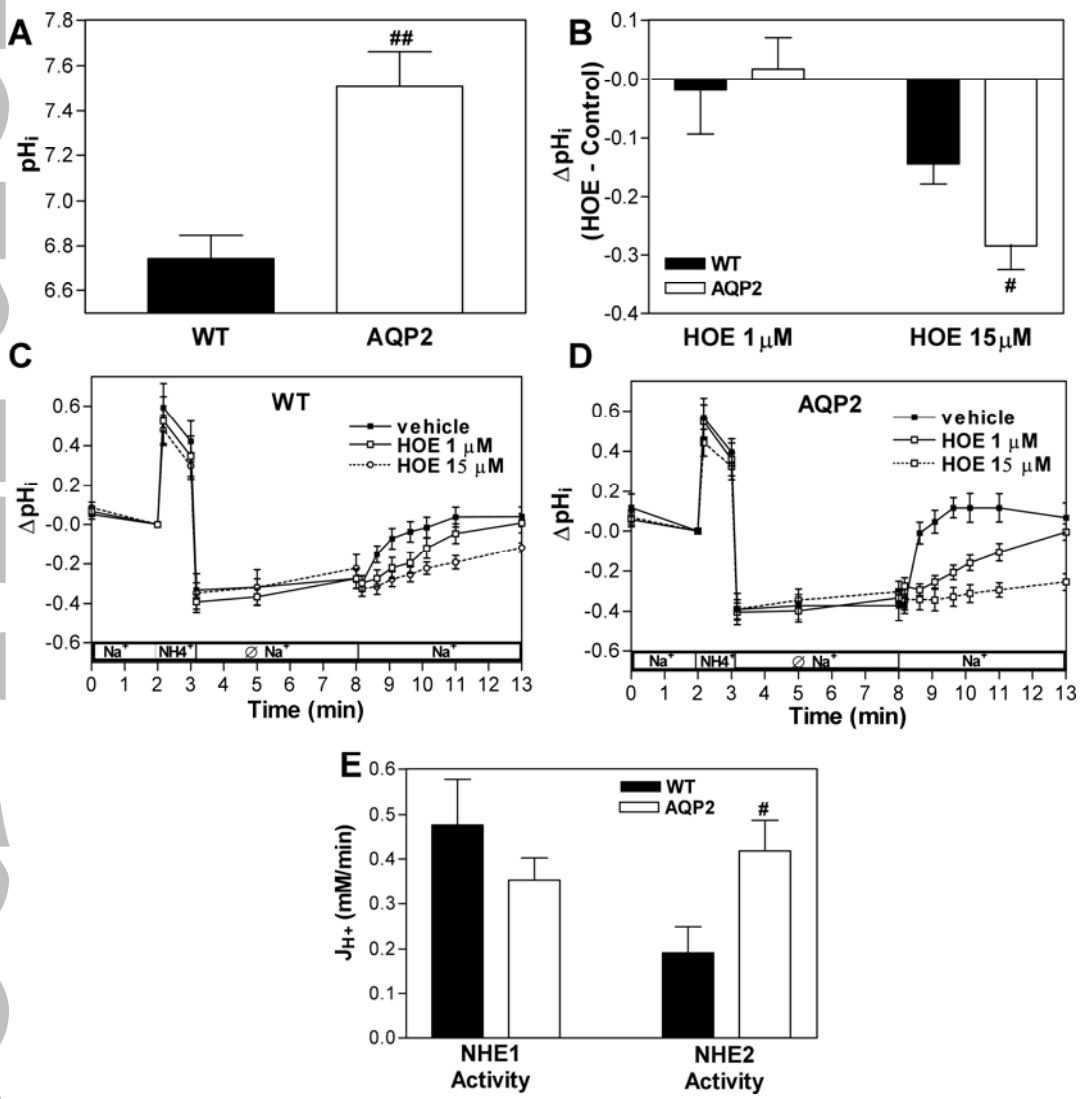

Figure 1

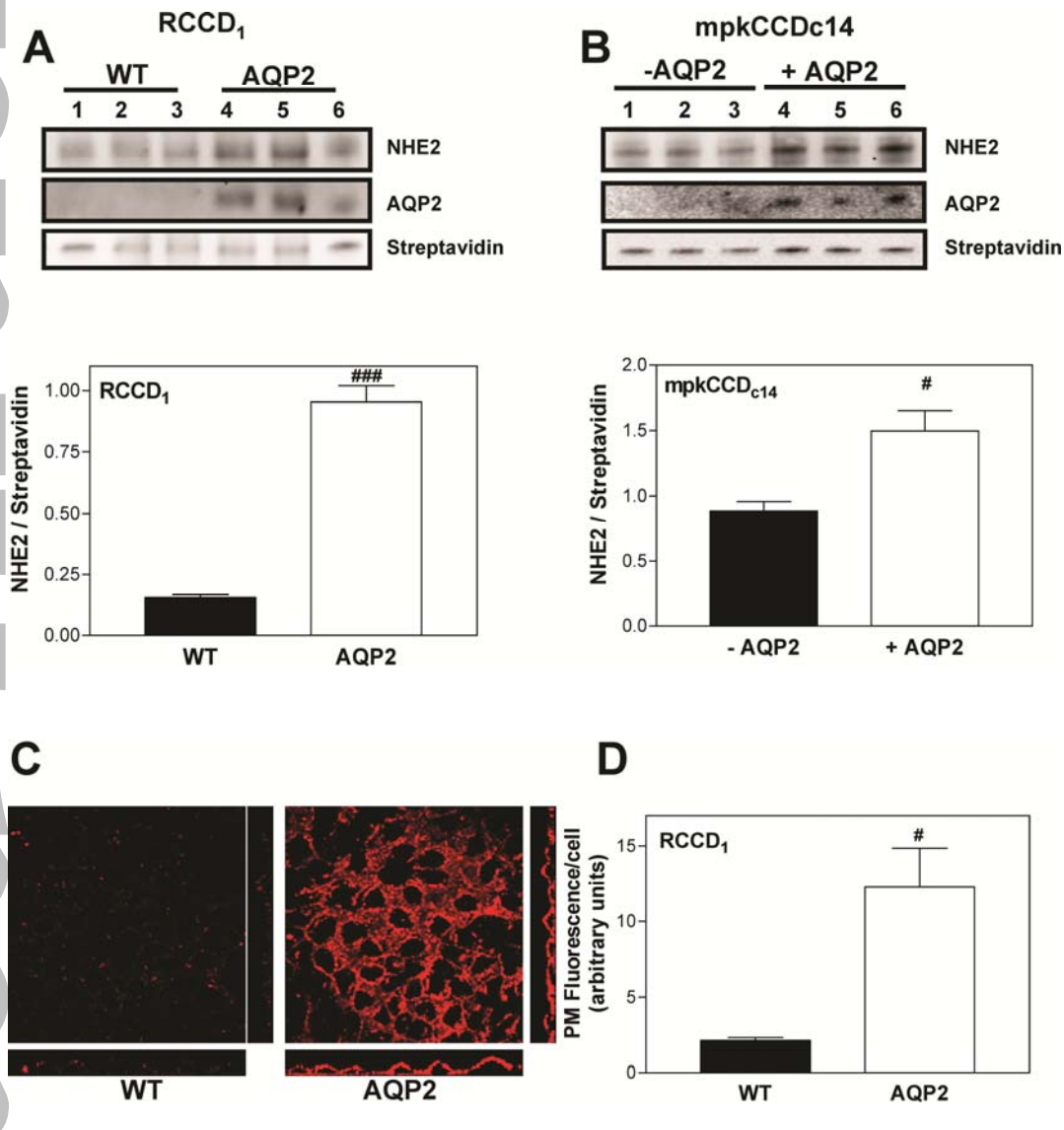

Figure 2

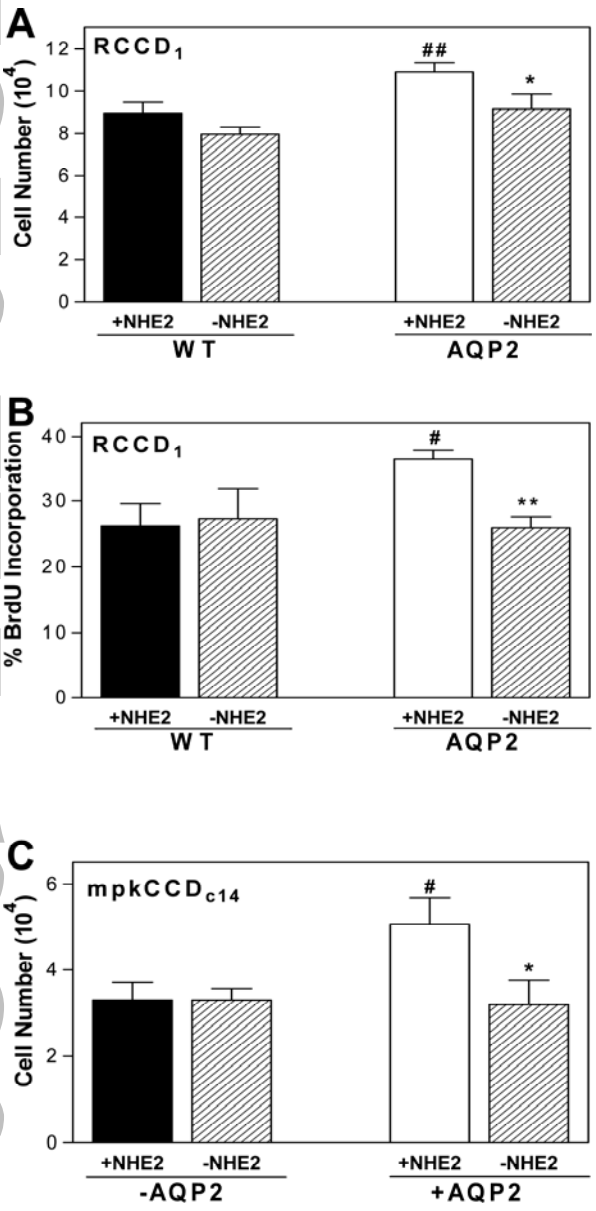

Figure 3

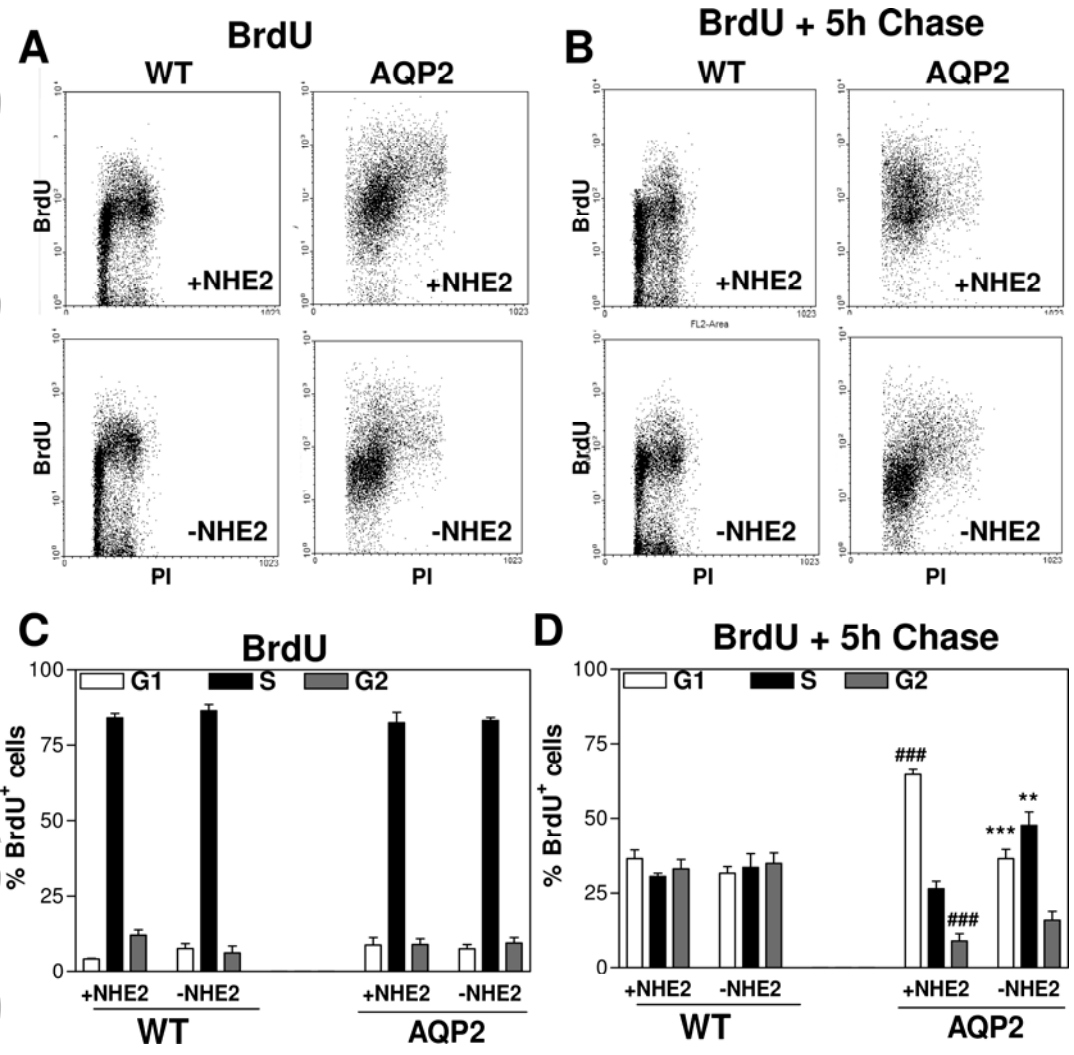

Figure 4

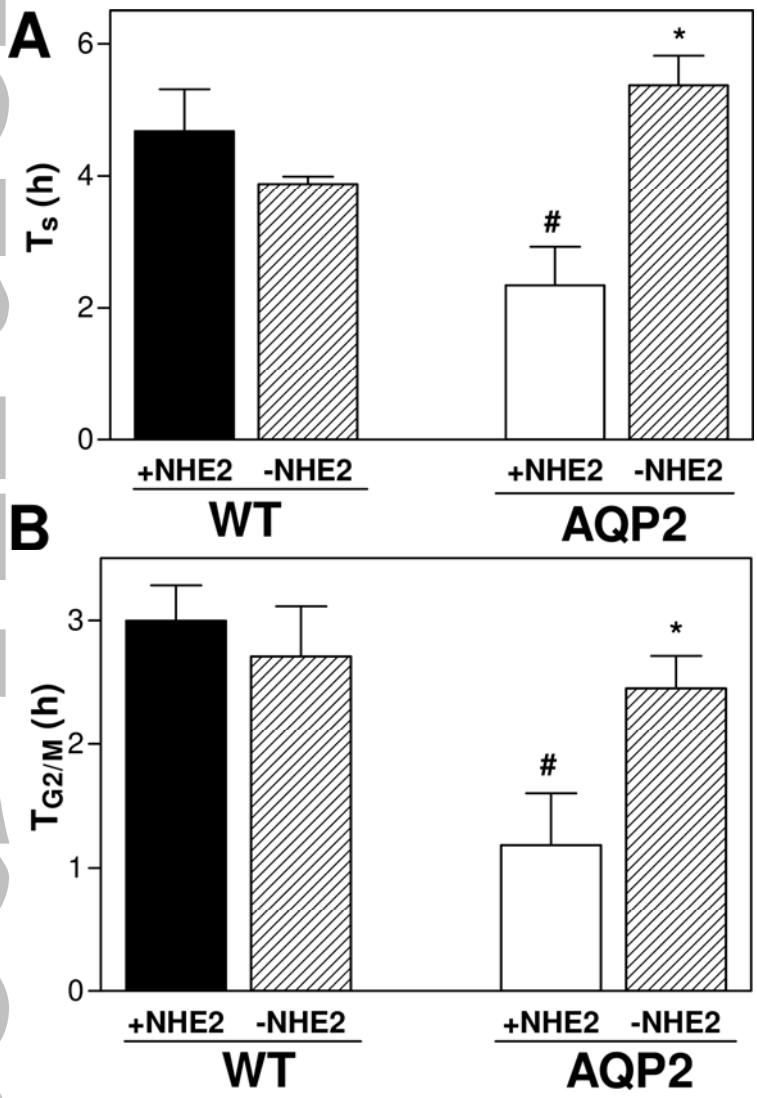

Figure 5

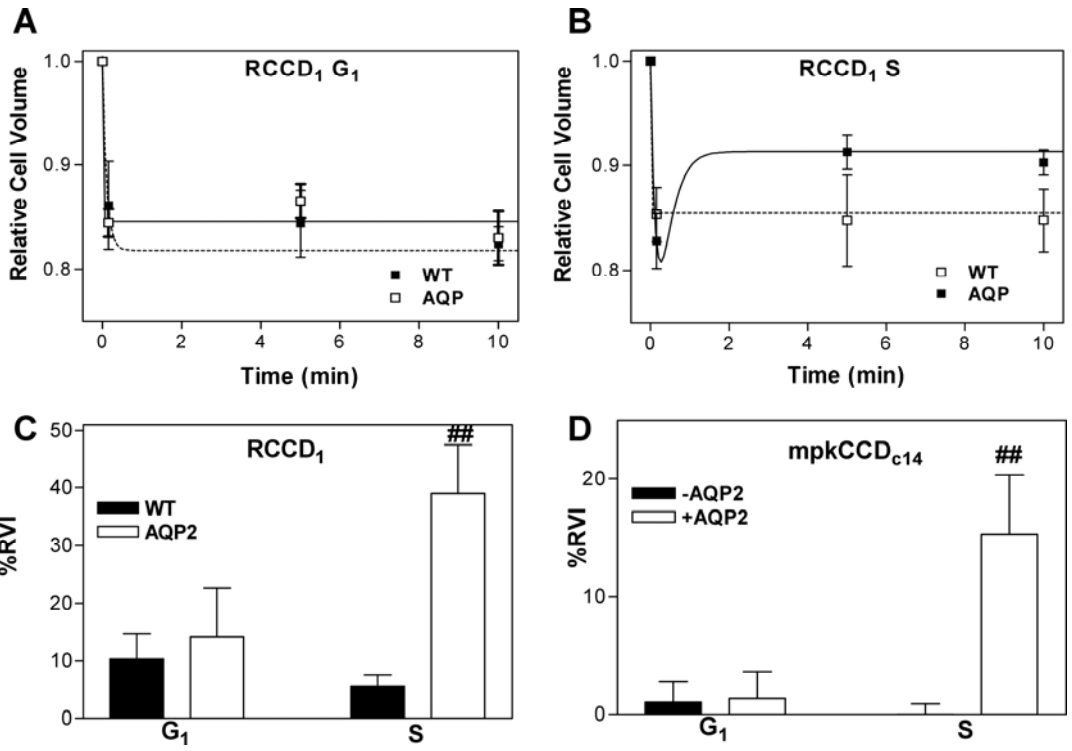

Figure 6